Cellular and Molecular Bioengineering, Vol. 15, No. 1, February 2022 *(© 2022)* pp. 15–29
https://doi.org/10.1007/s12195-021-00697-6

Original Article

Adipose Stroma Accelerates the Invasion and Escape of Human Breast Cancer Cells from an Engineered Microtumor

Yoseph W. Dance,[1] Tova Meshulam,[2,3] Alex J. Seibel,[1] Mackenzie C. Obenreder,[1] Matthew D. Layne,[3] Celeste M. Nelson,[4,5] and Joe Tien [1,6]

[1]Department of Biomedical Engineering, Boston University, 44 Cummington Mall, Boston, MA 02215, USA; [2]Boston Nutrition Obesity Research Center, Boston University School of Medicine, Boston, MA 02118, USA; [3]Department of Biochemistry, Boston University School of Medicine, Boston, MA 02118, USA; [4]Department of Chemical and Biological Engineering, Princeton University, 303 Hoyt Laboratory, William Street, Princeton, NJ 08544, USA; [5]Department of Molecular Biology, Princeton University, Princeton, NJ 08544, USA; and [6]Division of Materials Science and Engineering, Boston University, Boston, MA 02215, USA

(Received 29 April 2021; accepted 9 August 2021; published online 24 August 2021)

Associate Editor Michael R. King oversaw the review of this article.

Abstract

Introduction—Approximately 20–25% of human breast tumors are found within an adipose, rather than fibrous, stroma. Adipose stroma is associated with an increased risk of lymph node metastasis, but the causal association between adipose stroma and metastatic progression in human breast cancer remains unclear.

Methods—We used micropatterned type I collagen gels to engineer ~3-mm-long microscale human breast tumors within a stroma that contains adipocytes and adipose-derived stem cells (ASCs) (collectively, "adipose cells"). Invasion and escape of human breast cancer cells into an empty 120-μm-diameter lymphatic-like cavity was used to model interstitial invasion and vascular escape in the presence of adipose cell-derived factors for up to 16 days.

Results—We found that adipose cells hasten invasion and escape by 1–2 days and 2–3 days, respectively. These effects were mediated by soluble factors secreted by the adipose cells, and these factors acted directly on tumor cells. Surprisingly, tumor invasion and escape were more strongly induced by ASCs than by adipocytes.

Conclusions—This work reveals that both adipocytes and ASCs accelerate the interstitial invasion and escape of human breast cancer cells, and sheds light on the link between adipose stroma and lymphatic metastasis in human breast cancer.

Keywords—Triple-negative breast cancer, Intravasation, Lymphovascular invasion, Microphysiological system, Tumor engineering, Fat.

Address correspondence to Joe Tien, Department of Biomedical Engineering, Boston University, 44 Cummington Mall, Boston, MA 02215, USA; Celeste M. Nelson, Department of Chemical and Biological Engineering, Princeton University, 303 Hoyt Laboratory, William Street, Princeton, NJ 08544, USA. Electronic mails: celesten@princeton.edu, jtien@bu.edu

ABBREVIATIONS

ASC	Adipose-derived stem cell
ECM	Extracellular matrix
IFP	Interstitial fluid pressure

INTRODUCTION

Breast cancer metastasis, the spread of malignant breast cancer cells from a primary site and colonization at a secondary site, is associated with poor patient prognosis.[48] The metastatic cascade consists of invasion of tumor cells at a primary site into the surrounding stroma, vascular escape into a nearby blood or lymphatic vessel (intravasation), circulation through the vascular system, exit from the microvasculature (extravasation), and colony formation at a new site.[46] The human breast stroma consists of several cell types including adipocytes, adipose-derived stem cells (ASCs), fibroblasts, immune cells, and vascular (endothelial and mural) cells embedded in extracellular matrix (ECM). Stromal cells contribute to breast cancer progression through a variety of mechanisms including tumor angiogenesis, inflammation, and fibrosis.[11,12,28,35,54,59]

In human breast tumors, the stroma is classified histologically as fibrous (75–80% of cases) or adipose (20–25%).[32] Fibrous stroma exhibits increased colla-

gen deposition, collagen fiber alignment, and ECM stiffness, which drive breast tumor invasion.[1,14,24] Much less is known about how adipose stroma may affect breast cancer progression, even though adipose tissue is a major constituent of the human breast and surrounds the terminal ductal-lobular units where mammary carcinomas arise.[13,36,60] Breast tumors that are adjacent to adipose stroma have a higher risk of lymph node metastasis than tumors in a fibrous stroma do.[32] Obesity, which is associated with adipose tissue expansion, increases lymphovascular invasion and lymph node metastasis in breast cancer,[21,58] although other work suggests that body mass index (BMI) is not correlated with lymphatic metastasis in breast cancer.[20]

Previous studies that examined how adipocytes and ASCs affect breast cancer progression have focused mainly on the initial stages of tumor growth and invasion.[16] The number and size of adipocytes at the invasive front of human breast tumors *in vivo* are smaller than in uninvolved adipose tissue, which suggests that tumors induce lipolysis.[15] Indeed, human breast cancer cells enhance lipolysis *in vivo* and *in vitro*, liberating free fatty acids that increase the proliferation and migration of the cancer cells;[59] this effect is enhanced in cultures that contain obesity-associated adipocytes.[2] Human breast cancer cells that are cocultured with adipocytes undergo epithelial-mesenchymal transition (EMT), increase expression of vimentin, MMP-9, and Twist1, and acquire migratory phenotypes.[32] Breast cancer cells also induce neighboring adipocytes to secrete MMP-11 (stromelysin-3), which cleaves collagen VI and generates a proteolytic fragment that enhances breast cancer cell growth *in vitro*.[25,38] ASCs contribute to breast tumor progression through ECM remodeling and through secretion and deposition of cytokines.[7] These effects on the ECM are enhanced in ASCs from obese patients.[34,45]

Although it is recognized that adipocytes and ASCs (collectively, "adipose cells") affect breast tumor growth and local invasion of breast cancer cells, very little is known about how these cell types influence the subsequent escape of tumor cells into nearby blood or lymphatic vessels. Given that adipose cells increase invasion, do they cause a similar increase in escape? If so, are these effects mediated by physical or chemical signals, or both? Do adipocytes or ASCs play a larger role in adipose cell-associated escape? Tumor cell invasion and escape are distinct stages of metastasis, and signals that promote the former may not necessarily promote (and may even inhibit) the latter.[39] Here, we have engineered three-dimensional (3D) microfluidic models of human breast tumor aggregates in collagen gels to identify how adipose cells affect invasion and escape. Using a similar model, we have recently shown how interstitial fluid pressure (IFP), ECM concentration, matrix degradation, and breast cancer cell proliferation affect invasion and escape.[43,51–53] In the current study, we identified how cells in the stroma surrounding a tumor, particularly adipose cells, affect invasion and escape. We find that adipose cells secrete soluble factors that accelerate the invasion and escape of breast cancer cells, and that these factors act directly on tumor cells, rather than on the ECM. Invasion and escape are more strongly induced by ASC-derived factors, rather than by factors secreted by adipocytes. These data point to the resident cells in adipose tissue as key promoters of metastatic progression in human breast cancer.

MATERIALS AND METHODS

Cell Culture

MDA-MB-231 human breast carcinoma cells (lot #59704452; Physical Sciences-Oncology Network Bioresource Core Facility, ATCC) were cultured at 37 °C and 5% CO_2 in tumor medium (TM), which consisted of DMEM/F12 (Hyclone) supplemented with 10% heat-inactivated fetal bovine serum (FBS, lot #B18020; Atlanta Biologicals) and 50 μg/mL gentamicin (Sigma). These cells were routinely passaged at a 1:4 ratio through passage fifteen.

Human ASCs (Boston Nutrition Obesity Research Center) were grown from the stromal-vascular fraction (SVF) of subcutaneous adipose tissue discarded from bariatric surgery.[31] Briefly, minced adipose tissue was treated with collagenase solution (type 1, 1 mg/mL in Hanks' balanced salt solution (HBSS); Worthington Biochemical) and shaken at 100 rpm for 2 h at 37 °C. The digested tissue was filtered through a nylon mesh (mesh size 250 μm; Component Supply, Inc.). Cells that collected in the flow-through were centrifuged at $500\times g$ for 10 min at room temperature. Next, red blood cells in the cell pellets were lysed in 0.154 mM NH_4Cl, 10 mM K_2HPO_4 and 0.1 mM EDTA, pH 7.3. Finally, the washed cells were plated and cultured in growth medium (GM), which consisted of alpha-MEM (Gibco) supplemented with 10% FBS (Gemini Bio Products), 100 U/mL penicillin, and 10 μg/mL streptomycin (Pen/Strep; Corning). ASCs were isolated from a total of seven de-identified patients, and all comparisons used data that were obtained from ASCs of at least two patients (Supplementary Table 1).

Adipogenic differentiation of ASCs was induced two days post-confluence by replacing GM with serum-free complete differentiation medium (CDM), which consisted of DMEM/F12 (Gibco) supplemented with 25 mM sodium bicarbonate, 100 nM dexamethasone (Sigma), 1 μM rosiglitazone (Calbiochem),

100 nM insulin (Sigma), 0.5 mM 1-methyl-3-isobutylxanthine (IBMX; Sigma), 33 μM D-biotin (Sigma), 17 μM pantothenate (Sigma), 2 nM triiodo-L-thyronine (T_3; Sigma), 10 μg/mL transferrin (Sigma), and Pen/Strep.[31] CDM was replaced every 2–3 days.

On the seventh day of treatment with CDM, induced cultures were fed with maintenance medium (MM), which consisted of DMEM/F12 supplemented with sodium bicarbonate, Pen/Strep, 10 nM dexamethasone, 10 nM insulin, 33 μM D-biotin, 17 μM pantothenate, and 10 μg/mL transferrin. These cultures were refed with MM every three days for at least six additional days. Cultures that were differentiated and maintained for a total of 13–23 days (since the initial addition of CDM) were used for experiments. We refer to these cultures as "adipose cells"; although they consist mainly of adipocytes and residual undifferentiated ASCs, we acknowledge that some undifferentiated cells may be stromal fibroblasts.

As a positive control for CD31 expression, human dermal microvascular lymphatic endothelial cells (LECs; Promocell) were cultured on gelatin-coated dishes in MCDB131 medium (Caisson) supplemented with 10% FBS, 1% glutamine-penicillin-streptomycin (Invitrogen), 1 μg/mL hydrocortisone (Sigma), 80 μM dibutyryl cyclic AMP (Sigma), 25 μg/mL endothelial cell growth supplement (Alfa Aesar), 2 U/mL heparin (Sigma), and 0.2 mM ascorbic acid 2-phosphate (Sigma). As a positive control for CD45 expression, U937 human monocytes (ATCC) were cultured in RPMI medium (Gibco) supplemented with 10% FBS and 50 μg/mL gentamicin. Monocytes were not differentiated into macrophages before use.

Collection of Conditioned Medium

Adipose cell-conditioned medium was harvested by feeding 100-mm-diameter dishes of adipose cells with 10 mL of MM and collecting the medium three days later. Conditioned medium from undifferentiated ASCs was obtained by culturing ASCs to two days post-confluence, feeding them with 10 mL of MM, and collecting the medium three days later. All conditioned media were stored at 4 °C, supplemented with 3% FBS, and passed through a sterile syringe filter (0.2 μm; Corning) prior to use. Each batch of conditioned medium was collected from adipose cells or undifferentiated ASCs from a single donor.

Formation of Engineered Microtumors in Adipose Cell-Laden or Cell-Free Stroma

Microtumors (n = 225) in adipose cell-laden or cell-free stroma were formed by modifying an existing needle-based approach to mold microscale cavities in collagen gels (Fig. 1).[9,42,51] First, the interior walls of a 1 mm × 1 mm × 6 mm polydimethylsiloxane (PDMS) chamber were oxidized with UV/ozone, and the chamber was immediately placed upside-down onto a #1½ glass coverslip on a 100-mm-diameter dish and pre-coated with poly-D-lysine (300 kDa, 1 mg/mL in PBS; Sigma). Next, two stainless steel 120-μm-diameter needles (Seirin) were passivated with bovine serum albumin (1% in PBS; Calbiochem) and then aligned near the center of the PDMS chamber from opposite ends. Bovine dermal type I collagen (4.9 mg/mL, acid-extracted and not pepsin-treated, lot #210090; Koken) was neutralized with 0.2 M NaOH to a pH of 7 and diluted with 10× HBSS (Gibco), water, and TM to a collagen concentration of 3.9 mg/mL and an FBS concentration of 0.4%. Adipose cells from a 100-mm-diameter dish were trypsinized, removed from the dish by adding MM that was supplemented with 3% FBS, and centrifuged in this trypsin-media mixture at 1700 g for 10 min, yielding a large floating layer and a small pellet. The two fractions were combined to form a single cell suspension, and 8 μL of this suspension was added to 200 μL neutralized collagen to obtain a final density of ~10^5 cells/mL. For adipose cell-free stroma, 8 μL of TM was added to 200 μL neutralized collagen. In both adipose cell-laden and cell-free stroma, the final concentration of collagen was 3.75 mg/mL. Approximately 10 μL of collagen solution was transferred into each PDMS chamber. After 25 min of gelation at 37 °C, MM that was supplemented with 3% FBS was added to the two 6-mm-diameter wells adjacent to the gel. After at least thirty more minutes, needles were removed to yield two opposing blind-ended cavities that were separated by less than 200 μm (range 57–190 μm) at the center of the gel.

To form microtumors in a cell-laden stroma, we first fluorescently labeled MDA-MB-231 cells by washing them with PBS twice, treating them with PKH26 or PKH67 dye (2–10 μL/mL Diluent C; Sigma) for 1–3 min at room temperature, neutralizing unbound dye by adding TM, and washing them twice more with TM. MDA-MB-231 cells that were used in conditioned media experiments were not fluorescently labeled. We then added 70 μL of a dense suspension of MDA-MB-231 cells (1–2 × 10^6 cells/mL in MM that was supplemented with 3% FBS) to one well. Cells filled the cavity to generate a ~3-mm-long densely packed "microtumor"; the opposite cavity was left unseeded. Microtumors were refed every 10–14 h with MM or conditioned medium that contained 3% FBS for two days post-seeding by removing the media from both wells and adding ~70 μL to the well next to the tumor and ~60 μL to the opposite well. On day 2 post-seeding, a ~4-mm-thick PDMS spacer (made with a hole punch) was placed on the well opposite each micro-

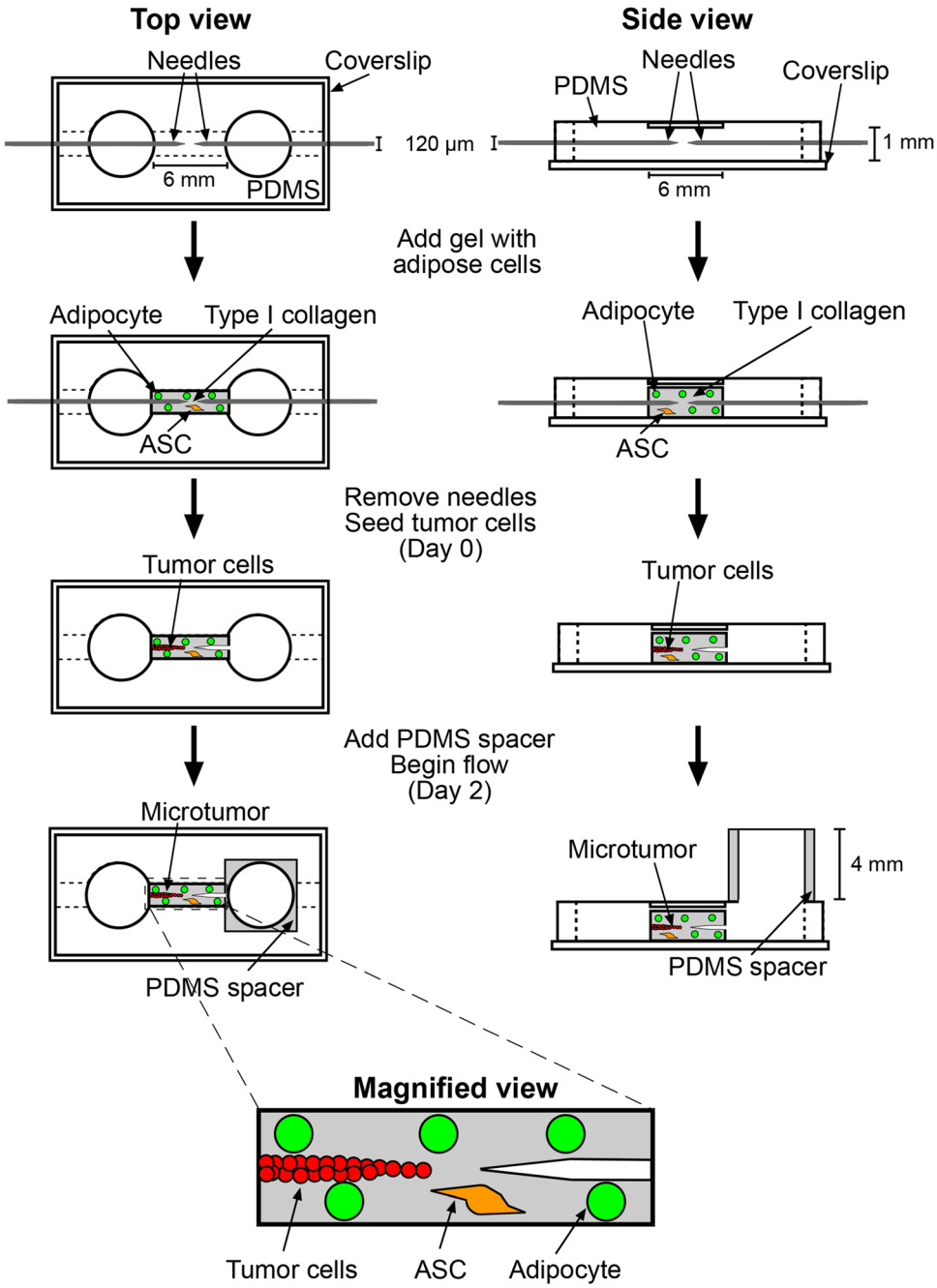

FIGURE 1. Schematic illustrating the formation of a ~3-mm-long 3D human breast microtumor and an empty 120-μm-diameter cavity within a ~6-mm-long adipose cell-laden gel.

tumor and filled with medium to generate a hydrostatic pressure head of ~6 mm H_2O. Prior work has shown that this pressure induces interstitial flow from the cavity to the tumor, which permits tumor cells to invade.[43,51–53] We continued to refeed tumors every 10–14 h by adding ~55 μL to the upstream well and removing ~45 μL of medium from the downstream well, for an additional two weeks (i.e., to day 16 post-seeding).

Assessment of Tumor Invasion and Escape

Phase-contrast images were acquired daily using an Axiovert 200 inverted microscope (Zeiss), 10×/0.30 *NA* Plan-Neofluar objective, and Axiocam MRm camera (Zeiss) at 1388 × 1040 resolution. Initial tumor-to-cavity distances were calculated as $\sqrt{D_{xy}{}^2 + D_z{}^2}$, where D_{xy} is the smallest two-dimensional in-plane distance between the microtumor and

cavity on the day of seeding, and D_z is the difference in height of the focal planes between the microtumor and cavity on the day of seeding. The difference in height was corrected by a factor of 1.33 to account for the index of refraction of the culture medium.

We used phase-contrast imaging and fluorescence imaging to determine when invasion and escape occurred. A tumor was considered to have invaded when at least one cell body was observed to be located at least ~20 μm from the initial boundary of the tumor. A tumor was considered to have escaped when at least one cell body was observed within the blind-ended cavity opposite the tumor. Microtumors that had not escaped by day 16 were discarded and considered censored on day 16 in the subsequent Kaplan-Meier analyses.

Measurement of Collagen Permeability

Solid collagen gels with or without embedded adipose cells (~10^5 cells/mL) were formed in PDMS scaffolds and placed under a hydrostatic pressure difference of ~15 mm H_2O using PDMS spacers that were filled with TM. The volume of TM that flowed across the gel in 1.5–2 h was measured. Darcy permeability (k) was calculated using the equation $k = Q\mu L/A\Delta P$, where Q is the volumetric flow rate, μ is the viscosity of TM (found to be 0.72 cPoise at 37 °C), L is the length of the gel, A is the cross-sectional area of the gel, and ΔP is the hydrostatic pressure difference.

Measurement of Collagen Elastic Modulus

Adipose cell-laden (~10^5 cells/mL) and cell-free collagen gels were cast between microscope slides to form gel discs of ~1 mm height and ~10 mm diameter. Each gel was submerged in PBS, before we carefully placed an aluminum ball (1.0 mm diameter; Precision Balls) on top of the gel and allowed it to deform the gel for one hour. The elastic modulus (E_{ind}) of each gel was calculated using the equation $E_{ind} = \pi R^{5/2}(\rho - \rho_{PBS})g/\delta^{3/2}$, where R is the radius of the ball (0.5 mm), ρ is the density of aluminum (2.7 g/cm^3), ρ_{PBS} is the density of PBS, g is gravitational acceleration (9.8 m/s^2), and δ is the indentation depth.

Immunofluorescence Staining

Microtumors in adipose cell-laden collagen were fixed by removing the media from both wells, removing the PDMS spacer, and adding ~80 μL of 4% paraformaldehyde (PF; Electron Microscopy Sciences) to the well adjacent to the tumor and ~20 μL to the opposite well for 15 min at room temperature on day 0 or day 7 post-seeding. These volumes were chosen to allow rapid fixation of the tumor.[42] Samples were permeabilized with a solution of 0.2% Triton X-100 (Sigma) and 5% goat serum (Invitrogen) for one hour; subsequent antibody and washing steps were performed in this buffer. Mouse antibody to cytokeratin (clone AE-1/AE-3; 5 μg/mL; Novus Biologicals) and rabbit polyclonal antibody to perilipin 1 (5 μg/mL; Invitrogen) were then introduced by adding ~80 μL of antibody solution to the well adjacent to the tumor and ~20 μL to the well opposite the tumor and allowing the solution to flow through the samples overnight at 4 °C. The next day, samples were washed three times for 20 min each. Alexa Fluor 594-conjugated goat anti-mouse (5 μg/mL; Invitrogen) and Alexa Fluor 488-conjugated goat anti-rabbit (5 μg/mL; Invitrogen) secondary antibodies and Hoechst 33342 (1 μg/mL; Invitrogen) were introduced by adding ~80 μL of labeled solution to the well adjacent to the tumor and ~20 μL to the well opposite the tumor and allowing the solution to flow through for one hour at room temperature. Samples were then washed with PBS three times for 20 min each. Some samples were further stained with Nile Red (1 μg/mL in PBS; Sigma) by adding ~80 μL of Nile Red solution to the well adjacent to the tumor and ~20 μL to the well opposite the tumor.

In other experiments, ASCs, LECs, and monocytes were cultured on glass coverslips and fixed by adding 4% PF for 15 min at room temperature. Cells were permeabilized with a solution of 0.2% Triton X-100 and 5% goat serum for one hour; subsequent antibody and washing steps were performed in this buffer. Rabbit polyclonal antibody to CD31 (0.45 μg/mL; Abcam) and mouse antibody to CD45 (clone 2D1; 0.63 μg/mL; BD Biosciences) were added to the slides and left overnight at 4 °C. The next day, samples were washed three times for 20 min each. Alexa Fluor 594-conjugated goat anti-mouse (5 μg/mL; Invitrogen) and Alexa Fluor 488-conjugated goat anti-rabbit (5 μg/mL; Invitrogen) secondary antibodies and Hoechst 33342 (1 μg/mL; Invitrogen) were added for one hour at room temperature. Samples were then washed with PBS three times for 20 min each.

Fluorescence images were acquired using an Axiovert 200 inverted microscope (Zeiss), 10×/0.30 *NA* Plan-Neofluar or 63×/0.95W Achroplan water immersion objective, and Axiocam MRm camera (Zeiss) at 1388 × 1040 resolution.

Statistics

Statistical tests were conducted using Graphpad Prism ver. 6. Invasion and escape curves were compared with the log-rank (Mantel-Cox) test. Comparison of cumulative frequency distributions for the starting tumor-to-cavity distance used the Kol-

mogorov-Smirnov test. Darcy permeability measurements were compared using two-way ANOVA. Indentation moduli were compared using the Mann-Whitney U test. A p value of less than 0.05 was considered to indicate a statistically significant difference.

RESULTS

Features of Engineered Microtumors in Adipose Cell-Laden Stroma

To determine how the combined presence of adipocytes and ASCs in the tumor microenvironment affect invasion and escape of breast cancer cells, we generated densely-packed aggregates of MDA-MB-231 breast cancer cells in adipose cell-laden collagen (Fig. 1). Since the stromal-vascular fraction (the cell population from which we obtained ASCs) also contains cells that lack the capacity to differentiate into adipocytes (primarily endothelial cells and leukocytes),[17] we stained ASCs before differentiation for the endothelial cell marker CD31 and the leukocyte marker CD45 (Fig. S1). This analysis revealed that $<0.2\%$ of the cells were CD31-positive, and $<0.3\%$ were CD45-positive.

We first characterized the 3D co-culture model on the day of seeding (day 0) with phase-contrast imaging and immunofluorescence staining (Fig. 2a). MDA-MB-231 cells were stained for cytokeratins, intermediate filament proteins that are characteristic of epithelial cells.[37] Adipocytes were stained for perilipin 1, a protein that localizes on the surface of intracellular lipid droplets.[3] Nuclei were stained with Hoechst 33342, and lipid droplets were further stained with Nile Red in some samples. As expected, cytokeratin staining was detected in breast cancer cells, while perilipin 1 staining outlined the perimeter of lipid droplets in adipocytes. Cells in the collagen gel that did not stain for adipocyte markers on day 0 after seeding were interpreted as residual ASCs, although these cells may possibly be other stromal cells (e.g., fibroblasts). Immunofluorescence staining revealed that ~92% of adipose cells on day 0 were adipocytes, and the remaining ~8% were ASCs. By day 7, a subset of adipocytes spread and adopted an elongated morphology in the gel, a finding that we attribute to partial adipocyte dedifferentiation, as reported by others (Fig. 2b).[49] Staining showed that, on day 7, ~65% of the adipose cells were adipocytes and ~35% were ASCs or dedifferentiated adipocytes.

Adipose Cells Promote Microtumor Invasion and Escape

In the presence of adipose cells, microtumors formed collective multicellular invasions at their periphery that extended into the collagen (Fig. 3a, *right*). Most invasions persisted throughout the duration of culture. Some microtumors in adipose cell-laden collagen invaded before the application of flow on day 2. While multicellular invasions also emerged from microtumors in adipose cell-free collagen, these invasions were often shorter and eventually overtaken by the growing breast cancer cell aggregate (Fig. 3a, *left*).

We used the Kaplan-Meier method to assess whether adipose cells alter the invasion and escape kinetics of PKH-labeled microtumors in collagen gels. We previously found that the initial (day 0) distance between the microtumor and cavity affects the rate of escape, with larger tumor-to-cavity distances resulting in slower escape but no difference in invasion.[43,52,53] Thus, we matched the distributions of initial tumor-to-cavity distances for microtumors in adipose cell-laden collagen and cell-free collagen ($p = 0.64$; Fig. S2a). Analysis of matched tumors revealed that invasions emerged 1–2 days earlier from microtumors in adipose cell-laden collagen compared to microtumors in adipose cell-free collagen ($p = 0.0011$; hazard ratio (HR) 2.7; 95% confidence interval (CI) 1.5–4.9; Fig. 3b). Microtumors in adipose cell-laden collagen escaped 2–3 days earlier than those in adipose cell-free collagen did ($p = 0.0057$; HR 2.3; 95% CI 1.3–4.3; Fig. 3c).

Adding adipose cells to the collagen gels can modify the physical properties (ECM stiffness, pore size) of the microenvironment around microtumors. For example, we have previously shown that incorporating 3T3-L1 mouse adipocytes decreases the elastic modulus of collagen, and others have shown that ASCs deposit ECM proteins including fibronectin that increase ECM stiffness.[33,45] The addition of 3T3-L1 mouse adipocytes also increases the hydraulic permeability of collagen gels.[33] Since ECM stiffness and pore size independently affect the invasion of breast cancer cells,[5,52] we measured the indentation moduli and Darcy permeability of collagen gels with and without embedded adipose cells. We found that the presence of adipose cells did not significantly alter the gel stiffness ($p = 0.44$; Fig. S3a), but increased the hydraulic permeability slightly ($p = 0.0076$; Fig. S3b). Since hydraulic permeability (k) and pore size can be related by the expression $k \sim (\textit{pore radius})^2$,[26] the ~10% increase in hydraulic permeability from the addition of adipose cells corresponds to a ~5% increase in average pore radius, an increase that is unlikely to be responsible for hastening of invasion and escape by adipose cells.[52] We therefore investigated the possibility that adipose cells

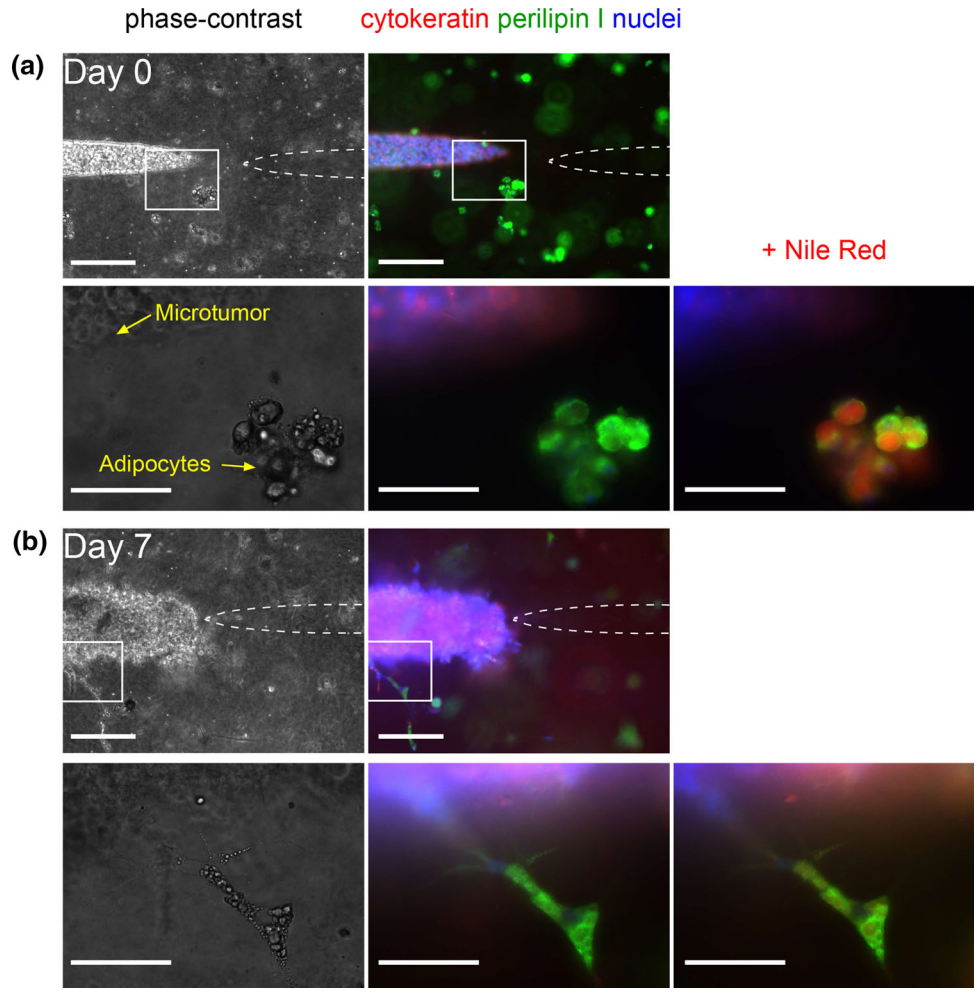

FIGURE 2. Phase-contrast (*left*) and immunofluorescence (*middle*, *right*) images of microtumors in adipose cell-laden collagen. Samples were stained for cytokeratin (*red*), perilipin 1 (*green*), and nuclei (*blue*) on (a) day 0 and (b) day 7 post-seeding, and then re-stained with Nile Red. Boxed areas (taken at 10× magnification) are magnified in the underlying images (taken at 63× magnification). Scale bars refer to 250 μm (*first row*, *third row*) and 75 μm (*second row*, *fourth row*). Images are from tumors with initial tumor-to-cavity distances of (a) 129 μm and (b) 95 μm.

altered the biochemical properties of the microenvironment.

Soluble Factors from Adipose Cells Promote Microtumor Invasion and Escape

Adipocytes and ASCs both produce many factors that promote breast tumor progression including adipokines, inflammatory cytokines, and matrix metalloproteinases (MMPs).[2,8,15,40,56] Since adipose cells caused modest changes in the physical properties of the collagen gels, we tested whether factors secreted from the adipose cells affected the behavior of breast cancer cells in our microtumor system. We formed microtumors in adipose cell-free collagen and exposed them to control or adipose cell-conditioned medium, starting on the day of seeding (i.e., on day 0). As before, the tumor-to-cavity distances were matched for microtumors that were treated with control or conditioned medium ($p = 0.99$; Fig. S2b).

Microtumors that were treated with conditioned medium displayed both single-cell and multicellular invasions (Fig. 4a, *right*), which persisted for up to two weeks. In contrast, only short multicellular invasions emerged in microtumors that were treated with control medium, and many of these invasions were overtaken by the breast cancer cell aggregate within a few days (Fig. 4a, *left*). Microtumors that were treated with conditioned medium invaded 1–2 days earlier ($p < 0.0001$; HR 11.3; 95% CI 4.9–26.0; Fig. 4b) and escaped 3–4 days earlier ($p < 0.0001$; HR 10.3; 95% CI 4.6–23.2; Fig. 4c) than those that were treated with control medium did. Occasionally, cancer cells that had escaped from tumors that were exposed to conditioned medium re-invaded the collagen. These results

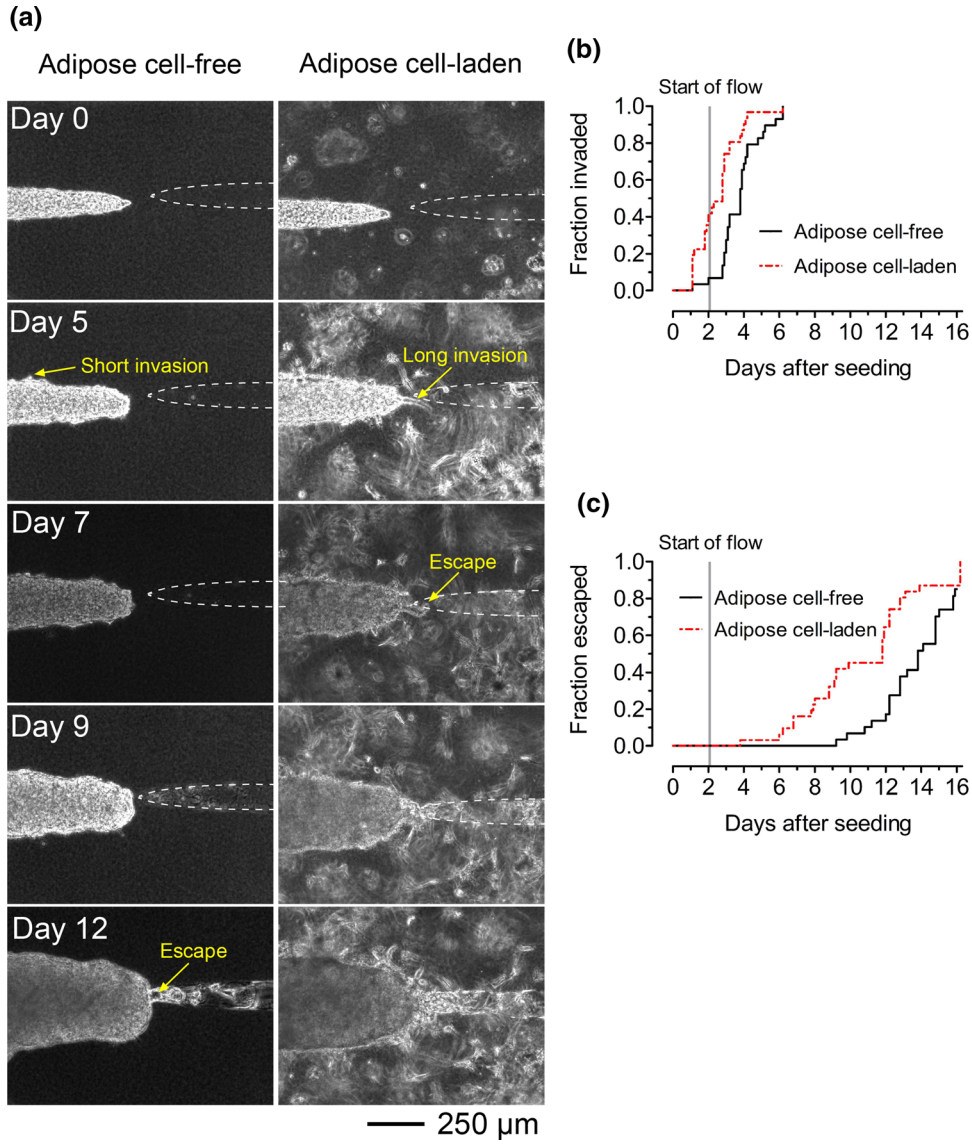

FIGURE 3. Adipose cell-laden collagen enhances invasion and escape of breast tumors. (a) Time-lapse phase-contrast images of tumors in adipose cell-free (*left*) and adipose cell-laden (*right*) collagen gels. Images are from tumors with initial tumor-to-cavity distances of 87 μm (adipose cell-free) and 95 μm (adipose cell-laden). (b) Invasion and (c) escape kinetics of microtumors in adipose cell-free and adipose cell-laden collagen.

reveal that adipose cells secrete soluble factors that enhance the invasion and escape of breast cancer cells.

Soluble Factors from Adipose Cells Promote Invasion and Escape by Acting Directly on Cancer Cells

Previous studies have shown that adipose cells secrete soluble factors, such as MMPs, that can degrade and remodel the ECM.[47,55] MMP-induced degradation can increase the ECM pore size, decrease the resistance of the ECM to cancer cell migration, and promote tumor invasion and escape.[43] To determine whether adipose cell-secreted soluble factors increase the pore size of the collagen, we treated unpatterned collagen gels with control or adipose cell-conditioned medium for up to six days. Darcy permeability measurements were performed after two, four, and six days of treatment. We found no significant difference in Darcy permeability in gels that were treated with control or conditioned medium ($p = 0.84$; Fig. S3c). This result suggests that soluble factors from adipose cells do not appreciably affect the pore size of the collagen gels.

In principle, adipose cell-secreted soluble factors such as TGF-β can bind to ECM proteins for subsequent interaction with tumor cells.[18] Thus, we investigated whether hastened invasion and escape in our model resulted from the deposition of soluble factors from adipose cell-conditioned medium in the collagen.

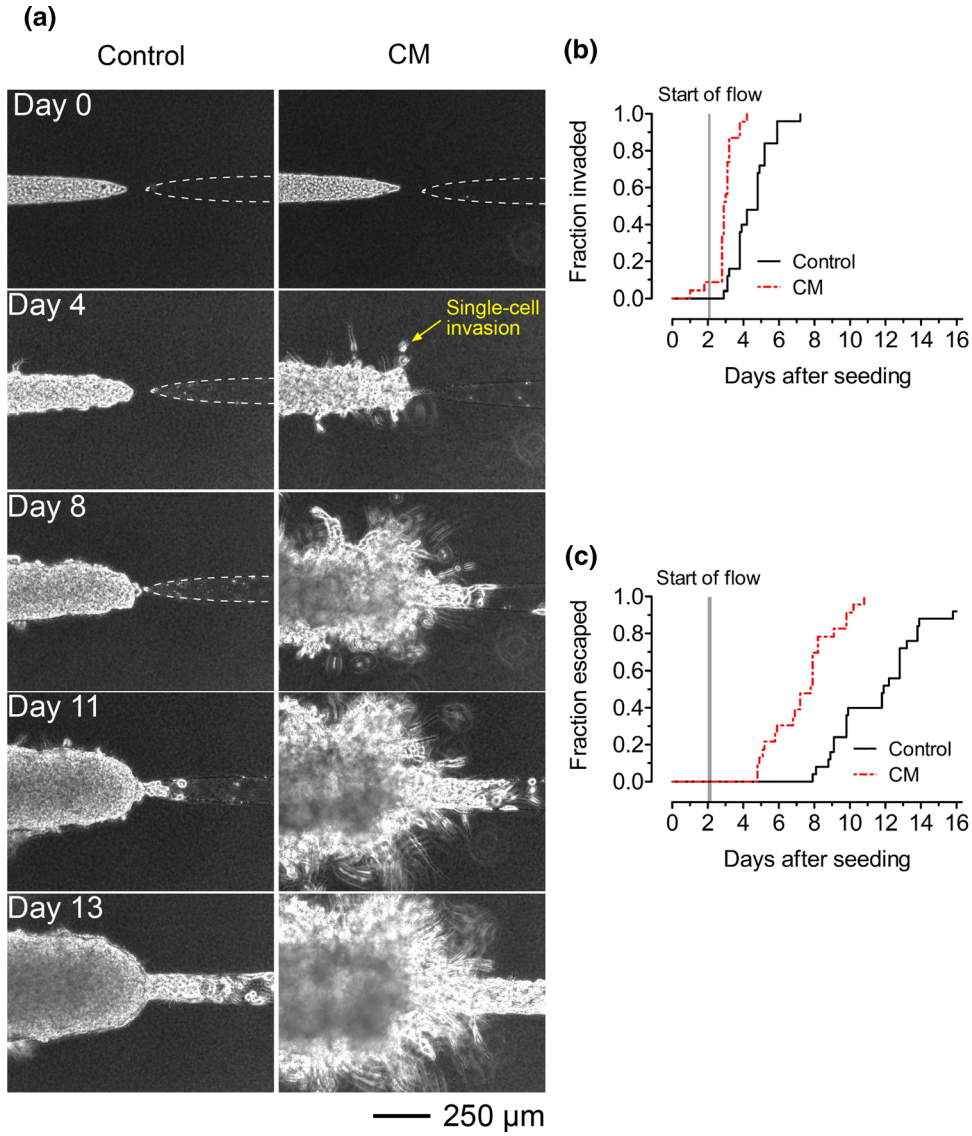

FIGURE 4. Adipose cell-conditioned medium hastens invasion and escape of tumors in cell-free collagen. (a) Time-lapse phase-contrast images of tumors in adipose cell-free collagen gels that were treated with control (*left*) or adipose cell-conditioned medium (*"CM"*; *right*). (b) Invasion and (c) escape kinetics of microtumors in adipose cell-free collagen that were treated with control or adipose cell-conditioned medium. Images are from tumors with initial tumor-to-cavity distances of 115 μm (control medium) and 79 μm (adipose cell-conditioned medium).

Prior to seeding tumor cells, we treated patterned, cell-free collagen gels with control or adipose cell-conditioned medium (CM) for four days. We then seeded tumor cells to form microtumors, which were then fed with either control or conditioned medium; all sets of tumors had matched tumor-to-cavity distances (p = 0.36–0.71 for pairwise comparisons; Fig. S2c). Strikingly, we found that tumors that were formed in conditioned medium-treated gels and then subsequently exposed to control medium (*"CM → control"*) behaved similarly to tumors in gels that were only treated and fed with control medium (*"control → control"*; Fig. 5a). These two sets of tumors invaded (p = 0.61; Fig. 5b) and escaped (p = 0.58; Fig. 5c) at similar rates. In contrast, tumors that were formed in conditioned medium-treated gels and then fed with conditioned medium (*"CM → CM"*) invaded ($p < 0.0001$; HR 6.0; 95% CI 2.5–14.0; Fig. 5b) and escaped ($p < 0.0001$; HR 7.9; 95% CI 3.4–18.1; Fig. 5c) sooner than *CM → control* tumors did. In other words, the pro-invasive effect of adipose cell-derived conditioned medium manifested only when microtumors were directly cultured in conditioned medium. Consistent with Fig. 4, *CM → CM* tumors invaded (p = 0.0001; HR 5.1; 95% CI 2.2–11.6; Fig. 5b) and escaped ($p < 0.0001$; HR 7.9; 95% CI 3.4–18.4; Fig. 5c) earlier than

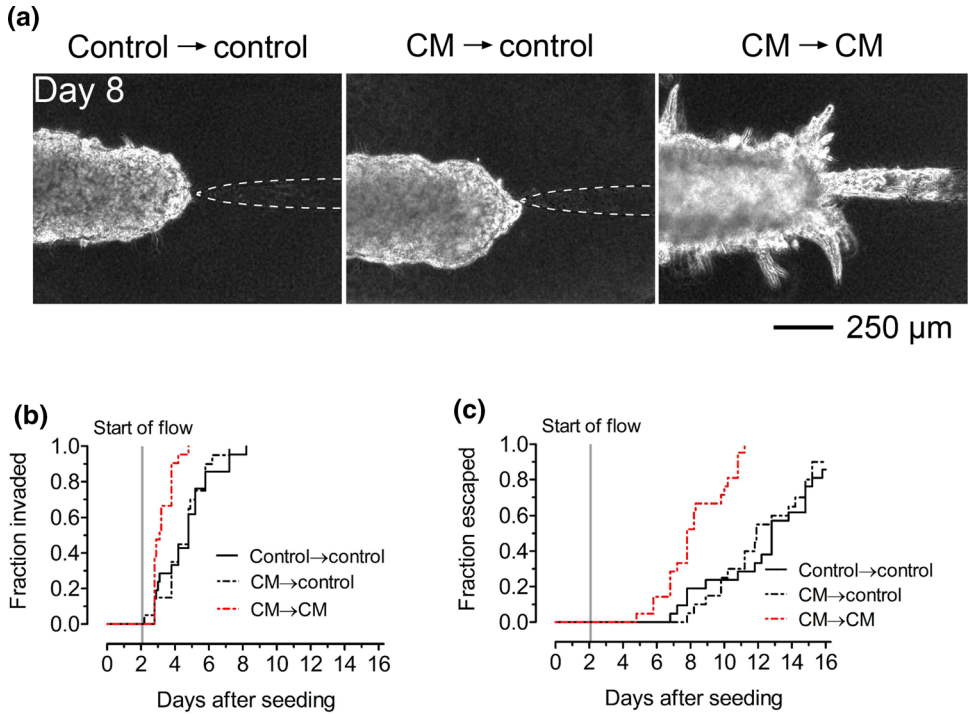

FIGURE 5. Adipose cell-conditioned medium accelerates invasion and escape by acting directly on tumor cells. (a) Phase-contrast images and (b) invasion and (c) escape kinetics of microtumors in adipose cell-free collagen gels that were previously treated with control medium or adipose cell-conditioned medium (*"CM"*). After seeding, tumors were fed either control medium or conditioned medium. *"Control → control"*, tumors that were formed in control medium-treated collagen and fed with control medium. *"CM → control"*, tumors that were formed in conditioned medium-treated collagen but fed with control medium. *"CM → CM"*, tumors that were formed in conditioned medium-treated collagen and fed with conditioned medium. Images are from tumors with initial tumor-to-cavity distances of 131 μm (*control → control*), 105 μm (*CM → control*), and 98 μm (*CM → CM*).

control → control tumors did. Altogether, our results suggest that adipose cell-conditioned medium contains soluble factors that hasten invasion and escape by directly acting on tumor cells, rather than by remodeling the collagen or by depositing factors in the matrix to indirectly promote invasion and escape.

ASC-Secreted Factors Promote Microtumor Invasion and Escape

To determine whether adipocytes or ASCs are primarily responsible for earlier invasion and escape, we compared microtumors that were treated with conditioned medium from adipose cells or from donor-matched undifferentiated ASCs. Microtumors in both conditions had similar tumor-to-cavity distances ($p = 0.79$; Fig. S2d). Microtumors that were treated with conditioned medium from undifferentiated ASCs displayed single-cell and multicellular invasions that persisted for up to two weeks (Fig. 6a). In fact, microtumors that were exposed to conditioned medium from undifferentiated ASCs invaded ($p < 0.0001$; HR 6.5; 95% CI 2.7–15.6; Fig. 6b) and escaped ($p = 0.0054$; HR 2.7; 95% CI 1.3–5.5; Fig. 6c) even earlier than those that were exposed to conditioned medium from adipose cells did. These results suggest that factors secreted by ASCs alone hasten the invasion and escape of breast cancer cells more than the factors secreted by mixtures of adipocytes and residual undifferentiated ASCs do.

DISCUSSION

Summary of Findings

In this study, we engineered a 3D model of human breast cancer invasion and escape through adipose stroma. Using this system, we found that adipose cells hasten the interstitial invasion and escape of MDA-MB-231 human breast cancer cells. Although the cavities into which the cancer cells escape are not lined by endothelium, the process of cell migration into a blind-ended cavity is intended to mimic lymphovascular escape. The effects that adipose cells exert on invasion and escape appear to be primarily mediated through adipose cell-derived soluble factors that act directly on tumor cells, rather than through ECM remodeling or by deposition of soluble factors in the

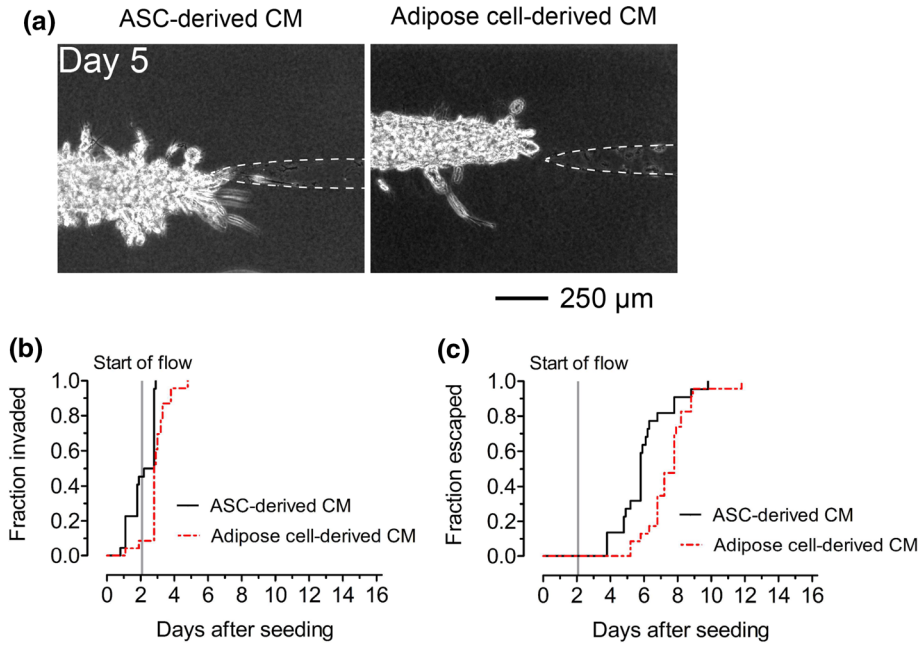

FIGURE 6. Soluble factors secreted by ASCs enhance invasion and escape to a greater extent than factors secreted by adipose cells do. (a) Phase-contrast images and (b) invasion and (c) escape kinetics of microtumors in adipose cell-free collagen gels that were treated with conditioned medium from ASCs or from adipose cells. Images are from tumors with initial tumor-to-cavity distances of 108 μm (ASC-derived conditioned medium) and 106 μm (adipose cell-derived conditioned medium).

ECM. Compared to adipose cells collectively, ASCs secrete factors that hasten invasion and escape to a greater extent.

Role of Adipose Cells in Breast Cancer Invasion and Escape

Adipose cells promote invasion of breast cancer cells through a variety of mechanisms.[16,23,34,59] Both adipocytes and ASCs can secrete invasion-promoting factors. For example, both can produce interleukin-6 (IL-6), which amplifies the invasion of human breast cancer cells *in vitro*.[15,56] Adipocyte-derived insulin-like growth factor binding protein-2 (IGFBP-2) stimulates the invasion of MCF-7 human breast cancer cells in Transwell models.[57] ASCs secrete the chemokine RANTES (CCL5), which promotes invasion of MDA-MB-231 cells.[41] Our findings show that MDA-MB-231 cells not only invade sooner, but they also escape earlier when exposed to adipose cell-conditioned medium. We note that the engineered model allows invasion and escape to occur in a 3D microenvironment, starting from a well-defined tumor, which resembles the *in vivo* situation.

The conditioned media from adipose cells and from ASCs both enhanced invasion and escape, with the latter being the more potent of the two. Since the adipose cells consisted primarily of adipocytes, these results suggest that ASCs promote tumor progression in the model tumors to a greater extent than adipocytes do. Although adipocytes can secrete soluble factors that hasten invasion and escape, they may secrete additional factors that inhibit these processes. For example, adiponectin is a well-studied adipokine that induces apoptosis and represses invasion of breast cancer cells.[29,44,50] The production of adiponectin increases with the extent of adipogenic differentiation.[27,62] The concentrations of invasion/escape-promoting factors may also be reduced as ASCs differentiate. For example, IL-6, TGF-β, and TGF-β-related proteins—which induce invasion and EMT[22,56]—are downregulated during adipogenesis.[4,30] We currently do not know which specific factor(s) mediate the effect of adipose cells in our breast cancer model, and we plan to use cytokine arrays and other biochemical approaches to identify these factor(s) in future work.

ASCs have also been reported to facilitate tumor progression through mechanical signaling. SVF-derived ASCs, particularly from obese mice, remodel and stiffen the surrounding ECM by depositing fibronectin.[45] This increased stiffness promotes mechanosensitive growth of MDA-MB-231 cells *in vitro*. In the current study, we did not detect changes in ECM stiffness with the addition of adipose cells, even though these cells were derived from obese (BMI 41.1 ± 2.0) donors. The adipose cells in our model consisted mainly of adipocytes, which have opposite effects on ECM stiffening compared to ASCs.[33,45] The low density of adipose cells that we used may not be

sufficiently high to generate appreciable differences in matrix stiffness. Other types of adipose-resident cells, such as endothelial cells and leukocytes, are present in our model in very small amounts ($< 0.5\%$ total), so it is statistically unlikely that the observed effects in our model are due to endothelial cells or leukocytes. Thus, we attribute the effects on invasion and escape to adipocytes and ASCs.

Comparison of Engineered Human Adipose Stroma to In Vivo Adipose Tissue

Our 3D engineered model of human breast cancer invasion and escape contains a stroma with the two characteristic cell types found in adipose tissue: adipocytes and ASCs. This model of stroma initially contains ~92% adipocytes and ~8% ASCs. Over time, a subset of adipocytes spread and appeared to partially dedifferentiate into ASC-like cells. In comparison, human subcutaneous adipose tissue is comprised of ~16% adipocytes and ~30% ASCs by cell number, with the remainder consisting of endothelial cells, leukocytes, fibroblasts, and smooth muscle cells.[17] By including adipocytes and ASCs as the only stromal cell types in our model, we were able to specifically assess how these cells together affect breast cancer cell invasion and escape in the absence of vascular or immune cell contributions. The density of adipose cells in the engineered model (~10^5 cells/mL) is roughly one order of magnitude lower than the density of adipocytes found *in vivo* (~10^6 cells/cm^3 tissue). In breast cancer, adipose stroma is defined to be $>50\%$ adipocytes by volume, and our stroma is well below that threshold. The lower cell density in our system facilitated imaging of the microtumor and adjacent cavity. Nevertheless, these differences should be kept in mind when assessing the relevance of our results to human breast cancer.

The collagen gels used in our model also differ from the native ECM of adipose tissue *in vivo*. The ECM of human adipose tissue consists of a variety of collagens, laminin, fibronectin, and elastin, while type I collagen is the main ECM protein in our model.[10,19] It is likely that the cells that are incorporated in the model eventually deposit additional ECM proteins. Moreover, while adipose tissue *in vivo* has a stiffness of ~2–10 kPa, our indentation moduli were much smaller (~50 Pa).[45,61] The physical properties of the type I collagen gels used in this engineered system permitted tumor cell invasion and escape to occur within a two week-long window. Future models can expand on this work to include additional ECM proteins native to adipose tissue.

CONCLUSIONS

The effects of the stroma in the stages of breast cancer progression up to intravasation have not been well-elucidated. Whether or not adipose tissue plays a pivotal role in lymphovascular escape remains unknown. This study revealed that the resident cells in adipose tissue accelerate the rate of breast cancer cell invasion and escape into a blind-ended cavity in the absence of endothelium. Both adipocytes and ASCs exerted these effects through cell-secreted factors. Numerous studies have identified factors in the secretomes of adipocytes and ASCs, many of which are found in the adipose tissue of high-risk breast cancer patients.[6,30,62,63] Subsequent work will refine this model by using ASCs derived from the human breast or from patients with a variety of metabolic phenotypes. We will build upon the existing model by studying intravasation into an endothelial cell-lined space, incorporating immune cells into the engineered stroma, and using cells of other subtypes besides triple-negative breast cancer.

SUPPLEMENTARY INFORMATION

The online version contains supplementary material available at https://doi.org/10.1007/s12195-021-00697-6.

ACKNOWLEDGMENTS

We thank Stephen Farmer (Boston Nutrition Obesity Research Center; BNORC) for insightful discussions. This study was funded by award U01 CA214292 from the National Cancer Institute and by award P30 DK046200 from the National Institute of Diabetes and Digestive and Kidney Diseases. Y.W.D. was supported by a training grant from the National Institute of General Medical Sciences (award T32 GM008764) and by a fellowship from the CURE Diversity Research Supplements Program at the National Cancer Institute. Human ASCs were provided by the Adipocyte Core of BNORC.

CONFLICT OF INTEREST

Yoseph W. Dance, Tova Meshulam, Alex J. Seibel, Mackenzie C. Obenreder, Matthew D. Layne, Celeste M. Nelson, and Joe Tien declare that they have no conflict of interest.

ETHICAL APPROVAL

No human or animal studies were carried out by the authors for this article.

REFERENCES

[1]Acerbi, I., L. Cassereau, I. Dean, Q. Shi, A. Au, C. Park, Y. Y. Chen, J. Liphardt, E. S. Hwang, and V. M. Weaver. Human breast cancer invasion and aggression correlates with ECM stiffening and immune cell infiltration. *Integr. Biol. (Camb.)* 7:1120–1134, 2015.

[2]Balaban, S., R. F. Shearer, L. S. Lee, M. van Geldermalsen, M. Schreuder, H. C. Shtein, R. Cairns, K. C. Thomas, D. J. Fazakerley, T. Grewal, J. Holst, D. N. Saunders, and A. J. Hoy. Adipocyte lipolysis links obesity to breast cancer growth: adipocyte-derived fatty acids drive breast cancer cell proliferation and migration. *Cancer Metab*. 5:1, 2017.

[3]Blanchette-Mackie, E. J., N. K. Dwyer, T. Barber, R. A. Coxey, T. Takeda, C. M. Rondinone, J. L. Theodorakis, A. S. Greenberg, and C. Londos. Perilipin is located on the surface layer of intracellular lipid droplets in adipocytes. *J. Lipid Res*. 36:1211–1226, 1995.

[4]Bortell, R., T. A. Owen, R. Ignotz, G. S. Stein, and J. L. Stein. TGF-β_1 prevents the down-regulation of type I procollagen, fibronectin, and TGF-β_1 gene expression associated with 3T3-L1 pre-adipocyte differentiation. *J. Cell. Biochem*. 54:256–263, 1994.

[5]Butcher, D. T., T. Alliston, and V. M. Weaver. A tense situation: forcing tumour progression. *Nat. Rev. Cancer* 9:108–122, 2009.

[6]Celis, J. E., J. M. Moreira, T. Cabezón, P. Gromov, E. Friis, F. Rank, and I. Gromova. Identification of extracellular and intracellular signaling components of the mammary adipose tissue and its interstitial fluid in high risk breast cancer patients: toward dissecting the molecular circuitry of epithelial-adipocyte stromal cell interactions. *Mol. Cell. Proteomics* 4:492–522, 2005.

[7]Chandler, E. M., B. R. Seo, J. P. Califano, R. C. Andresen Eguiluz, J. S. Lee, C. J. Yoon, D. T. Tims, J. X. Wang, L. Cheng, S. Mohanan, M. R. Buckley, I. Cohen, A. Y. Nikitin, R. M. Williams, D. Gourdon, C. A. Reinhart-King and C. Fischbach. Implanted adipose progenitor cells as physicochemical regulators of breast cancer. *Proc. Natl. Acad. Sci. USA* 109:9786-9791, 2012.

[8]Choi, J., Y. J. Cha, and J. S. Koo. Adipocyte biology in breast cancer: from silent bystander to active facilitator. *Prog. Lipid Res*. 69:11–20, 2018.

[9]Chrobak, K. M., D. R. Potter, and J. Tien. Formation of perfused, functional microvascular tubes in vitro. *Microvasc. Res*. 71:185–196, 2006.

[10]Chun, S. Y., J. O. Lim, E. H. Lee, M. H. Han, Y. S. Ha, J. N. Lee, B. S. Kim, M. J. Park, M. Yeo, B. Jung, and T. G. Kwon. Preparation and characterization of human adipose tissue-derived extracellular matrix, growth factors, and stem cells: a concise review. *Tissue Eng. Regen. Med*. 16:385–393, 2019.

[11]Colpaert, C., P. Vermeulen, E. Van Marck, and L. Dirix. The presence of a fibrotic focus is an independent predictor of early metastasis in lymph node-negative breast cancer patients. *Am. J. Surg. Pathol*. 25:1557–1558, 2001.

[12]Costa, A., Y. Kieffer, A. Scholer-Dahirel, F. Pelon, B. Bourachot, M. Cardon, P. Sirven, I. Magagna, L. Fuhrmann, C. Bernard, C. Bonneau, M. Kondratova, I. Kuperstein, A. Zinovyev, A. M. Givel, M. C. Parrini, V. Soumelis, A. Vincent-Salomon, and F. Mechta-Grigoriou. Fibroblast heterogeneity and immunosuppressive environment in human breast cancer. *Cancer Cell* 33:463–479, 2018.

[13]D'Esposito, V., M. R. Ambrosio, M. Giuliano, S. Cabaro, C. Miele, F. Beguinot, and P. Formisano. Mammary adipose tissue control of breast cancer progression: impact of obesity and diabetes. *Front Oncol*. 10:1554, 2020.

[14]DeFilippis, R. A., H. Chang, N. Dumont, J. T. Rabban, Y. Y. Chen, G. V. Fontenay, H. K. Berman, M. L. Gauthier, J. Zhao, D. Hu, J. J. Marx, J. A. Tjoe, E. Ziv, M. Febbraio, K. Kerlikowske, B. Parvin, and T. D. Tlsty. CD36 repression activates a multicellular stromal program shared by high mammographic density and tumor tissues. *Cancer Discov*. 2:826–839, 2012.

[15]Dirat, B., L. Bochet, M. Dabek, D. Daviaud, S. Dauvillier, B. Majed, Y. Y. Wang, A. Meulle, B. Salles, S. Le Gonidec, I. Garrido, G. Escourrou, P. Valet, and C. Muller. Cancer-associated adipocytes exhibit an activated phenotype and contribute to breast cancer invasion. *Cancer Res*. 71:2455–2465, 2011.

[16]Duong, M. N., A. Geneste, F. Fallone, X. Li, C. Dumontet, and C. Muller. The fat and the bad: mature adipocytes, key actors in tumor progression and resistance. *Oncotarget* 8:57622–57641, 2017.

[17]Eto, H., H. Suga, D. Matsumoto, K. Inoue, N. Aoi, H. Kato, J. Araki, and K. Yoshimura. Characterization of structure and cellular components of aspirated and excised adipose tissue. *Plast. Reconstr. Surg*. 124:1087–1097, 2009.

[18]Flaumenhaft, R., and D. B. Rifkin. The extracellular regulation of growth factor action. *Mol. Biol. Cell* 3:1057–1065, 1992.

[19]Flynn, L. E. The use of decellularized adipose tissue to provide an inductive microenvironment for the adipogenic differentiation of human adipose-derived stem cells. *Biomaterials* 31:4715–4724, 2010.

[20]Gao, Y., X. Chen, Q. He, R. C. Gimple, Y. Liao, L. Wang, R. Wu, Q. Xie, J. N. Rich, K. Shen, and Z. Yuan. Adipocytes promote breast tumorigenesis through TAZ-dependent secretion of resistin. *Proc. Natl. Acad. Sci. USA* 117:33295–33304, 2020.

[21]Gillespie, E. F., M. E. Sorbero, D. A. Hanauer, M. S. Sabel, E. J. Herrmann, L. J. Weiser, C. H. Jagielski, and J. J. Griggs. Obesity and angiolymphatic invasion in primary breast cancer. *Ann. Surg. Oncol*. 17:752–759, 2010.

[22]Hao, Y., D. Baker, and P. Ten Dijke. TGF-β-mediated epithelial-mesenchymal transition and cancer metastasis. *Int. J. Mol. Sci*. 20:2767, 2019.

[23]Hume, R. D., L. Berry, S. Reichelt, M. D'Angelo, J. Gomm, R. E. Cameron, and C. J. Watson. An engineered human adipose/collagen model for in vitro breast cancer cell migration studies. *Tissue Eng. Part A* 24:1309–1319, 2018.

[24]Huo, C. W., G. Chew, P. Hill, D. Huang, W. Ingman, L. Hodson, K. A. Brown, A. Magenau, A. H. Allam, E. McGhee, P. Timpson, M. A. Henderson, E. W. Thompson, and K. Britt. High mammographic density is associated with an increase in stromal collagen and immune cells within the mammary epithelium. *Breast Cancer Res*. 17:79, 2015.

[25]Iyengar, P., V. Espina, T. W. Williams, Y. Lin, D. Berry, L. A. Jelicks, H. Lee, K. Temple, R. Graves, J. Pollard, N. Chopra, R. G. Russell, R. Sasisekharan, B. J. Trock, M. Lippman, V. S. Calvert, E. F. Petricoin, L. Liotta, E. Dadachova, R. G. Pestell, M. P. Lisanti, P. Bonaldo, and P. E. Scherer. Adipocyte-derived collagen VI affects early mammary tumor progression in vivo, demonstrating a critical interaction in the tumor/stroma microenvironment. *J. Clin. Invest*. 115:1163–1176, 2005.

[26]Jackson, G. W., and D. F. James. The permeability of fibrous porous media. *Can. J. Chem. Eng*. 64:364–374, 1986.

[27]Jager, M., M. J. Lee, C. Li, S. R. Farmer, S. K. Fried and M. D. Layne. Aortic carboxypeptidase-like protein enhances adipose tissue stromal progenitor differentiation into myofibroblasts and is upregulated in fibrotic white adipose tissue. *PLoS ONE* 13:e0197777, 2018.

[28]Kakolyris, S., S. B. Fox, M. Koukourakis, A. Giatromanolaki, N. Brown, R. D. Leek, M. Taylor, I. M. Leigh, K. C. Gatter, and A. L. Harris. Relationship of vascular maturation in breast cancer blood vessels to vascular density and metastasis, assessed by expression of a novel basement membrane component, LH39. *Br. J. Cancer* 82:844–851, 2000.

[29]Kang, J. H., Y. Y. Lee, B. Y. Yu, B. S. Yang, K. H. Cho, D. K. Yoon, and Y. K. Roh. Adiponectin induces growth arrest and apoptosis of MDA-MB-231 breast cancer cell. *Arch. Pharm. Res*. 28:1263–1269, 2005.

[30]Kim, J., Y. S. Choi, S. Lim, K. Yea, J. H. Yoon, D. J. Jun, S. H. Ha, J. W. Kim, J. H. Kim, P. G. Suh, S. H. Ryu, and T. G. Lee. Comparative analysis of the secretory proteome of human adipose stromal vascular fraction cells during adipogenesis. *Proteomics* 10:394–405, 2010.

[31]Lee, M. J., and S. K. Fried. Optimal protocol for the differentiation and metabolic analysis of human adipose stromal cells. *Methods Enzymol*. 538:49–65, 2014.

[32]Lee, Y., W. H. Jung, and J. S. Koo. Adipocytes can induce epithelial-mesenchymal transition in breast cancer cells. *Breast Cancer Res. Treat*. 153:323–335, 2015.

[33]Li, X., J. Xia, C. T. Nicolescu, M. W. Massidda, T. J. Ryan and J. Tien. Engineering of microscale vascularized fat that responds to perfusion with lipoactive hormones. *Biofabrication* 11:014101, 2019.

[34]Ling, L., J. A. Mulligan, Y. Ouyang, A. A. Shimpi, R. M. Williams, G. F. Beeghly, B. D. Hopkins, J. A. Spector, S. G. Adie, and C. Fischbach. Obesity-associated adipose stromal cells promote breast cancer invasion through direct cell contact and ECM remodeling. *Adv. Funct. Mater*. 30:1910650, 2020.

[35]Mao, Y., E. T. Keller, D. H. Garfield, K. Shen, and J. Wang. Stromal cells in tumor microenvironment and breast cancer. *Cancer Metastasis Rev*. 32:303–315, 2013.

[36]Mertz, D., J. Sentosa, G. Luker, and S. Takayama. Studying adipose tissue in the breast tumor microenvironment in vitro: progress and opportunities. *Tissue Eng. Regen. Med*. 17:773–785, 2020.

[37]Moll, R., W. W. Franke, D. L. Schiller, B. Geiger, and R. Krepler. The catalog of human cytokeratins: patterns of expression in normal epithelia, tumors and cultured cells. *Cell* 31:11–24, 1982.

[38]Motrescu, E. R., S. Blaise, N. Etique, N. Messaddeq, M. P. Chenard, I. Stoll, C. Tomasetto, and M. C. Rio. Matrix metalloproteinase-11/stromelysin-3 exhibits collagenolytic function against collagen VI under normal and malignant conditions. *Oncogene* 27:6347–6355, 2008.

[39]Padmanaban, V., I. Krol, Y. Suhail, B. M. Szczerba, N. Aceto, J. S. Bader, and A. J. Ewald. E-cadherin is required for metastasis in multiple models of breast cancer. *Nature* 573:439–444, 2019.

[40]Pallegar, N. K., and S. L. Christian. Adipocytes in the tumour microenvironment. *Adv. Exp. Med. Biol*. 1234:1–13, 2020.

[41]Pinilla, S., E. Alt, F. J. Abdul Khalek, C. Jotzu, F. Muehlberg, C. Beckmann and Y. H. Song. Tissue resident stem cells produce CCL5 under the influence of cancer cells and thereby promote breast cancer cell invasion. *Cancer Lett*. 284:80-85, 2009.

[42]Piotrowski-Daspit, A. S., A. K. Simi, M. F. Pang, J. Tien, and C. M. Nelson. A 3D culture model to study how fluid pressure and flow affect the behavior of aggregates of epithelial cells. *Methods Mol. Biol*. 1501:245–257, 2017.

[43]Rabie, E. M., S. X. Zhang, A. P. Kourouklis, A. N. Kilinc, A. K. Simi, D. C. Radisky, J. Tien, and C. M. Nelson. Matrix degradation and cell proliferation are coupled to promote invasion and escape from an engineered human breast microtumor. *Integr. Biol. (Camb.)*. 13:17–29, 2021.

[44]Schäffler, A., J. Schölmerich, and C. Buechler. Mechanisms of disease: adipokines and breast cancer - endocrine and paracrine mechanisms that connect adiposity and breast cancer. *Nat. Clin. Pract. Endocrinol. Metab*. 3:345–354, 2007.

[45]Seo, B. R., P. Bhardwaj, S. Choi, J. Gonzalez, R. C. Andresen Eguiluz, K. Wang, S. Mohanan, P. G. Morris, B. Du, X. K. Zhou, L. T. Vahdat, A. Verma, O. Elemento, C. A. Hudis, R. M. Williams, D. Gourdon, A. J. Dannenberg and C. Fischbach. Obesity-dependent changes in interstitial ECM mechanics promote breast tumorigenesis. *Sci. Transl. Med*. 7:301ra130, 2015.

[46]Seyfried, T. N., and L. C. Huysentruyt. On the origin of cancer metastasis. *Crit. Rev. Oncog*. 18:43–73, 2013.

[47]Song, Y. H., S. H. Shon, M. Shan, A. D. Stroock, and C. Fischbach. Adipose-derived stem cells increase angiogenesis through matrix metalloproteinase-dependent collagen remodeling. *Integr. Biol. (Camb.)*. 8:205–215, 2016.

[48]Stebbing, J., and S. Ngan. Breast cancer (metastatic). *BMJ Clin. Evid*. 2010:0811, 2010.

[49]Sugihara, H., N. Yonemitsu, S. Toda, S. Miyabara, S. Funatsumaru, and T. Matsumoto. Unilocular fat cells in three-dimensional collagen gel matrix culture. *J. Lipid Res*. 29:691–697, 1988.

[50]Taliaferro-Smith, L., A. Nagalingam, D. Zhong, W. Zhou, N. K. Saxena, and D. Sharma. LKB1 is required for adiponectin-mediated modulation of AMPK-S6K axis and inhibition of migration and invasion of breast cancer cells. *Oncogene* 28:2621–2633, 2009.

[51]Tien, J., J. G. Truslow and C. M. Nelson. Modulation of invasive phenotype by interstitial pressure-driven convection in aggregates of human breast cancer cells. *PLoS ONE* 7:e45191, 2012.

[52]Tien, J., U. Ghani, Y. W. Dance, A. J. Seibel, M. Karakan, K. L. Ekinci and C. M. Nelson. Matrix pore size governs escape of human breast cancer cells from a microtumor to an empty cavity. *iScience* 23:101673, 2020.

[53]Tien, J., Y. W. Dance, U. Ghani, A. J. Seibel, and C. M. Nelson. Interstitial hypertension suppresses escape of human breast tumor cells via convection of interstitial fluid. *Cell. Mol. Bioeng*. 14:147–159, 2021.

[54]Tiwari, P., A. Blank, C. Cui, K. Q. Schoenfelt, G. Zhou, Y. Xu, G. Khramtsova, F. Olopade, A. M. Shah, S. A. Khan, M. R. Rosner, and L. Becker. Metabolically activated

adipose tissue macrophages link obesity to triple-negative breast cancer. *J. Exp. Med.* 216:1345–1358, 2019.
[55]Tokunaga, M., M. Inoue, Y. Jiang, R. H. Barnes, D. A. Buchner, and T. H. Chun. Fat depot-specific gene signature and ECM remodeling of $Sca1^{high}$ adipose-derived stem cells. *Matrix Biol.* 36:28–38, 2014.
[56]Walter, M., S. Liang, S. Ghosh, P. J. Hornsby, and R. Li. Interleukin 6 secreted from adipose stromal cells promotes migration and invasion of breast cancer cells. *Oncogene* 28:2745–2755, 2009.
[57]Wang, C., C. Gao, K. Meng, H. Qiao and Y. Wang. Human adipocytes stimulate invasion of breast cancer MCF-7 cells by secreting IGFBP-2. *PLoS ONE* 10:e0119348, 2015.
[58]Wang, J., Y. Cai, F. Yu, Z. Ping, and L. Liu. Body mass index increases the lymph node metastasis risk of breast cancer: a dose-response meta-analysis with 52904 subjects from 20 cohort studies. *BMC Cancer* 20:601, 2020.
[59]Wang, Y. Y., C. Attané, D. Milhas, B. Dirat, S. Dauvillier, A. Guerard, J. Gilhodes, I. Lazar, N. Alet, V. Laurent, S. Le Gonidec, D. Biard, C. Hervé, F. Bost, G. S. Ren, F. Bono, G. Escourrou, M. Prentki, L. Nieto, P. Valet and C. Muller. Mammary adipocytes stimulate breast cancer invasion through metabolic remodeling of tumor cells. *JCI Insight* 2:e87489, 2017.
[60]Wellings, S. R., H. M. Jensen, and R. G. Marcum. An atlas of subgross pathology of the human breast with special reference to possible precancerous lesions. *J. Natl. Cancer Inst.* 55:231–273, 1975.
[61]Yuan, Y., J. Gao and R. Ogawa. Mechanobiology and mechanotherapy of adipose tissue-effect of mechanical force on fat tissue engineering. *Plast. Reconstr. Surg. Glob. Open* 3:e578, 2015.
[62]Zhong, J., S. A. Krawczyk, R. Chaerkady, H. Huang, R. Goel, J. S. Bader, G. W. Wong, B. E. Corkey, and A. Pandey. Temporal profiling of the secretome during adipogenesis in humans. *J. Proteome Res.* 9:5228–5238, 2010.
[63]Zvonic, S., M. Lefevre, G. Kilroy, Z. E. Floyd, J. P. DeLany, I. Kheterpal, A. Gravois, R. Dow, A. White, X. Wu, and J. M. Gimble. Secretome of primary cultures of human adipose-derived stem cells: modulation of serpins by adipogenesis. *Mol. Cell. Proteomics* 6:18–28, 2007.

Supplementary Table 1: Demographic and clinical data for the ASC donors in this study. All patients were non-diabetic.

Patient	Age	Sex	BMI	Ethnicity / Race
1	45	Female	41.1	Black
2	42	Female	41.4	White, non-Hispanic
3	30	Female	43.0	Black
4	37	Female	40.8	NA
5	43	Female	41.7	Hispanic
6	33	Female	36.9	Black
7	40	Female	42.5	White, non-Hispanic

BMI, body mass index. NA, not available.

Supplementary Figure 1: Phase-contrast (*left*) and immunofluorescence (*right*) images of cells on coverslips. (a) CD31 (*green*) and nuclei (*blue*) stains of LECs and ASCs. (b) CD45 (*red*) and nuclei (*blue*) stains of monocytes and ASCs.

Supplementary Figure 2: Relative cumulative frequency distributions of initial (day 0) tumor-to-cavity distances. (a) For tumors in adipose cell-laden and cell-free collagen gels (Fig. 3). (b) For tumors in adipose cell-free collagen gels, treated with control or adipose cell-conditioned medium (Fig. 4). (c) For tumors that were formed in adipose cell-free collagen gels pretreated in control medium and fed with control medium (*"control → control"*), in gels pretreated in conditioned medium and fed with control medium (*"CM → control")*, and in gels pretreated in conditioned medium and fed with conditioned medium (*"CM → CM"*) (Fig. 5). (d) For tumors in adipose cell-free collagen gels treated with conditioned medium from ASCs or adipose cells (Fig. 6).

Supplementary Figure 3: Physical properties of collagen gels. (a) Indentation modulus of adipose cell-free and adipose cell-laden collagen gels. (b) Darcy permeability of adipose cell-free and adipose cell-laden collagen gels. (c) Darcy permeability of adipose cell-free collagen gels that were treated with control or adipose cell-conditioned medium.

Supplementary Figure 1:

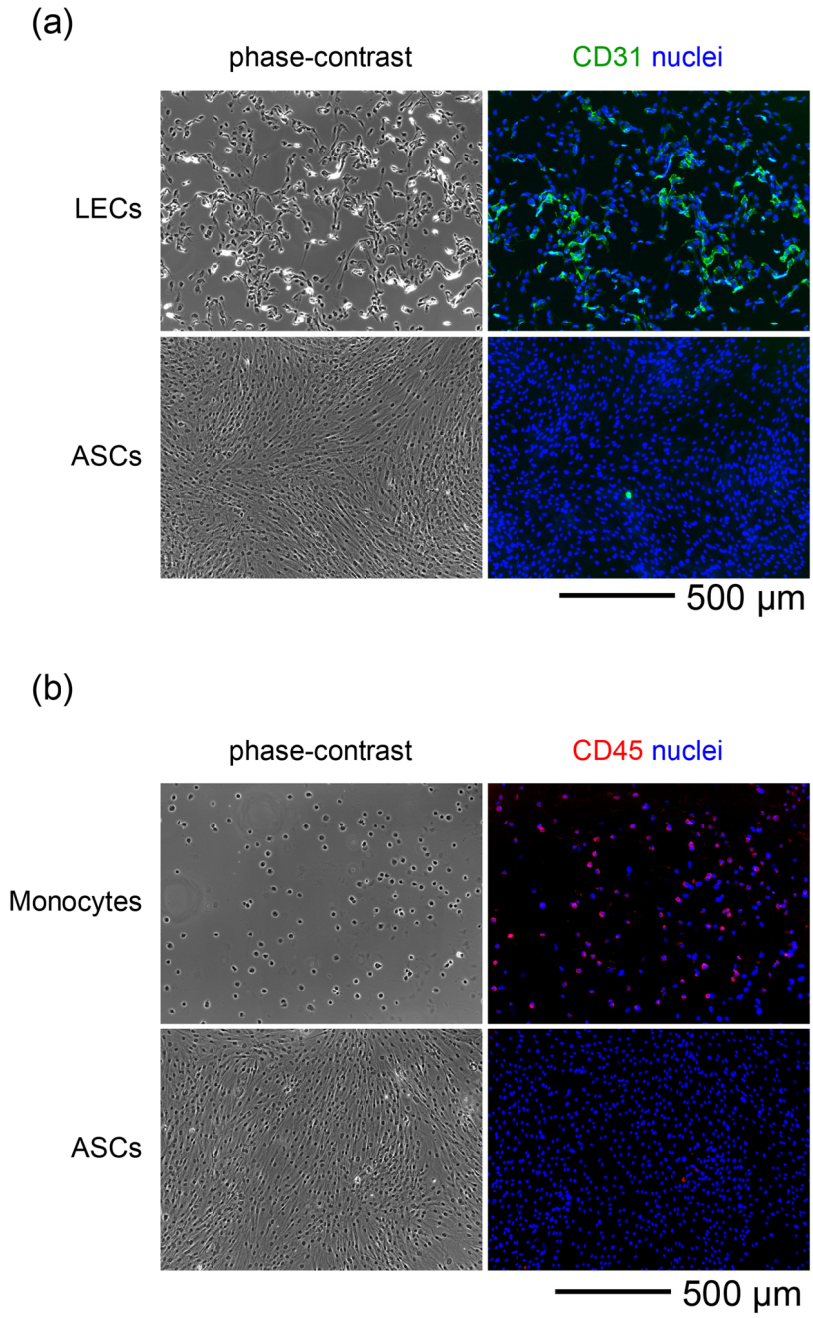

Supplementary Figure 2:

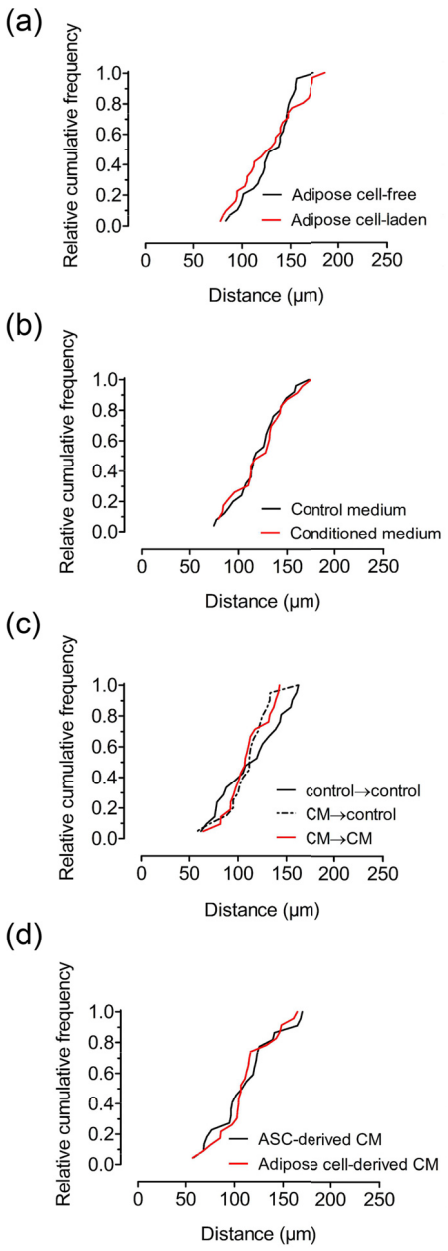

Supplementary Figure 3: